

Binary radiopulsar, as a laboratory of fundamental physics

G.S.Bisnovatyi-Kogan

(IKI, Moscow and JINR, Dubna)

1. Pulsars and close binaries
2. Hulse-Taylor pulsar
3. Disrupted pulsar pairs
4. RP statistics
5. Enhanced evaporation: formation of single RP
6. GR Effects: NS+NS
7. A Double-Pulsar System
8. Checking General Relativity
9. GW from NS merging
10. Variability of the gravitational constant.

Discovery of pulsars: A.Hewish, J.Bell et al., 1968, Nature, 217, 709

1973: all pulsars are single (more than 100)

more than half massive stars (predecessors of pulsars) are in binaries.

Possible explanations: pair disruption during explosion

no possibility to form a radiopulsar in pairs

1971: X-ray satellite UHURU

Discovery of X-ray pulsars in binaries.

Her X-1: X ray pulsar

Period of pulsations $P(p)=1.24$ sec, orbital $P(orb)=1.7$ days

Neutron star mass 1.4 Solar masses

Optical star mass about 2 Solar masses

This system should give birth to the binary radiopulsar

Bisnovatyi-Kogan G.S. and Komberg B.V., 1974, *Astron. Zh.* **51**,373

Reasons:

1. After 100 million years the optical star will become a white dwarf, mass transfer will be finished, and the system will be transparent to radio emission.
2. X ray pulsar is accelerating its rotation due to accretion, so after the birth of the white dwarf companion the neutron star will rotate rapidly, $P(p)$ about 100 msec.

Question:

Why are the binary radiopulsars not found (1973) ?

Answer (B-K, K, 1974):

Because the magnetic field of the neutron star is decreasing about 100 times during the accretion, so binary radiopulsars are very faint objects,

Pulsar luminosity $L \sim B^2/P^4$

At small B luminosity L is low even at the rapid rotation

Magnetic field is screened by the infalling plasma

Pulsars and close binary systems

G. S. Bisnovatyi-Kogan and B. V. Komberg

Institute of Applied Mathematics,

Academy of Sciences of the USSR

(Submitted April 27, 1973)

Astron. Zh., 51, 373-381 (March-April 1974)

The absence of radio pulsars from binary systems might be attributable to a decay in the magnetic field of a neutron-star binary component as accretes material from the primary star. Thus even after accretion ceases and radio waves are no longer absorbed, the neutron-star component would not be observable as a radio pulsar. An analysis of the accelerated rotation of the x-ray pulsar Her X-1, which belongs to a close binary, also implies a weaker magnetic field ($B \ll 10^{10}$ gauss) than in radio pulsars. The evolution of a close binary whose components have nearly equal masses is considered qualitatively. The more massive star may be the first to explode as a supernova, followed by disruption of the binary system. Soon the companion should also explode as the two stars will have evolved concurrently. This situation could produce a pair of radio pulsars located close together. The space distribution of radio pulsars is examined; several pairs of nearby pulsars at high galactic latitudes are identified. An observational test is proposed for the hypothesis that such pairs originate from the disruption of a binary: The magnitude and direction of their peculiar velocity would be measured.

We therefore see that evolutionary considerations certainly do not preclude the possibility that a neutron star might be found paired with another star also in a terminal evolutionary stage (white dwarf, neutron star, "collapsar"); on the contrary, they point to such a conclusion with high probability. Hence the absence of radio pulsars from close binary systems requires, as we have indicated at the beginning of Sec. 3, a further assumption regarding the decay of the magnetic field.

DISCOVERY OF A PULSAR IN A BINARY SYSTEM

R. A. HULSE AND J. H. TAYLOR

THE ASTROPHYSICAL JOURNAL, 195:L51-L53, 1975 January 15

Received 1974 October 18

PARAMETERS OF THE BINARY PULSAR

$$\begin{aligned}\alpha(1950.0) &= 19^{\text{h}}13^{\text{m}}13^{\text{s}} \pm 4^{\text{s}} \\ \delta(1950.0) &= +16^{\circ}00'24'' \pm 60'' \\ l &= 49^{\circ}9 \\ b &= 2^{\circ}1 \\ P_{\text{cm}} &= 0^{\text{s}}059030 \pm 0^{\text{s}}000001 \\ dP_{\text{cm}}/dt &< 1 \times 10^{-12} \\ \text{DM} &= 167 \pm 5 \text{ cm}^{-3} \text{ pc} \\ S_{430} &= 0.006 \pm 0.003 \text{ Jy} \\ W_e &< 10 \text{ ms}\end{aligned}$$

ELEMENTS OF THE ORBIT

$$\begin{aligned}K_1 &= 199 \pm 5 \text{ km s}^{-1} \\ P_b &= 27908 \pm 7 \text{ s} \\ e &= 0.615 \pm 0.010 \\ \omega &= 179^{\circ} \pm 1^{\circ} \\ T &= \text{JD } 2,442,321.433 \pm 0.002 \\ a_1 \sin i &= 1.00 \pm 0.02 R_{\odot} \\ f(m) &= 0.13 \pm 0.01 M_{\odot}\end{aligned}$$

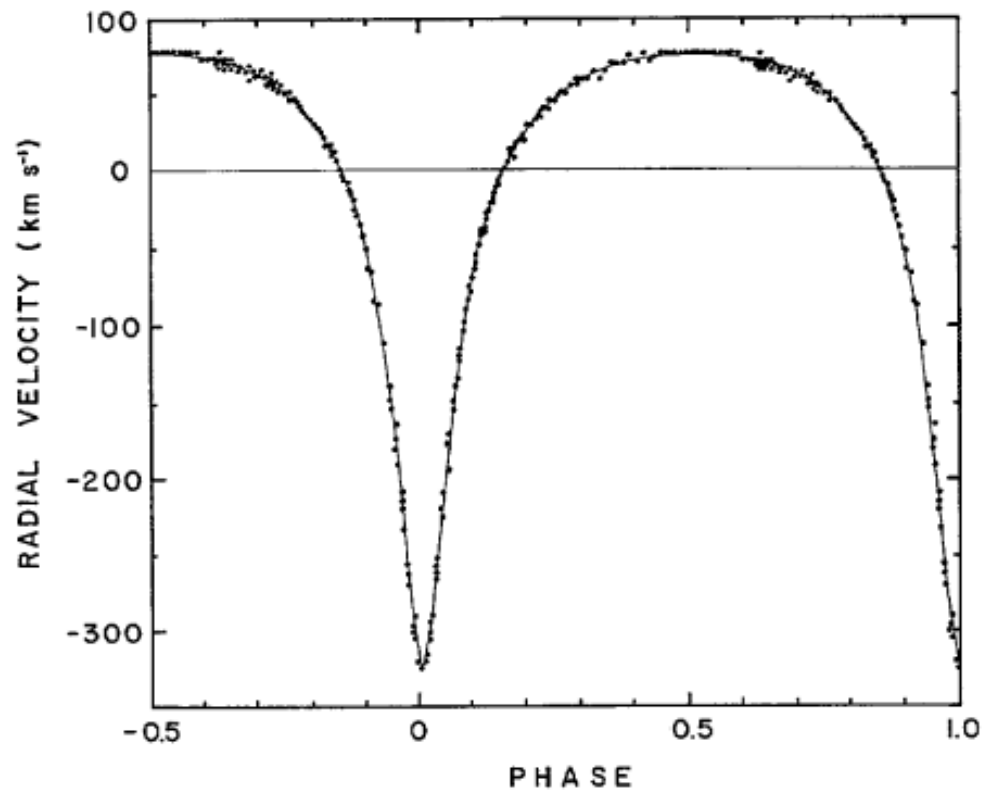


FIG. 1.—Velocity curve for the binary pulsar. Points represent measurements of the pulsar period distributed over parts of 10 different orbital periods. The curve corresponds to equations (1)–(4), with parameters from table 2.

Physics Today
1975, 28, No.11,
pp. 46-54

Informal discussion
at Landau Theor. Inst.

Left to right:

G.S.Bisnovatyi-Kogan,
I.D.Novikov,
Academicians
V.L.Ginzburg and
Ya.B.Zeldovich, and
David Pines.
(Photo G.Baym)



The properties of the first binary pulsar coincide with our predictions:
Rapid rotation and **Small magnetic field**

Possible evolution of a binary-system radio pulsar as an old object with a weak magnetic field

G. S. Bisnovatyi-Kogan and B. V. Komberg

Pis'ma Astron. Zh. 2, 338–342 (July 1976)

Taylor et al.³ have recently reported measurements of \dot{P}_{rot} for PSR 1913 + 16, which has the anomalously small value $\dot{P}_{\text{rot}} = (8.8 \pm 0.3) \cdot 10^{-18}$ for its value of P_{rot} . Knowing \dot{P}_{rot} for PSR 1913 + 16, we can readily estimate its rate of rotational-energy loss,

$$\dot{E} = -I\Omega\dot{\Omega} = I \left(\frac{2\pi}{P_{\text{rot}}} \right)^2 \frac{\dot{P}_{\text{rot}}}{P_{\text{rot}}} = 2 \cdot 10^{33} \text{ erg/sec},$$

$$B_s = \left(\frac{3Ic^3 P_{\text{rot}} \dot{P}_{\text{rot}}}{8\pi^2 R_{\text{NS}}^6} \right)^{1/4} \approx 2.3 \cdot 10^{10} \text{ gauss},$$

The average magnetic fields of single radiopulsars is about 10^{12} Gauss.

2008: New class of neutron stars: recycled pulsars, more than 180 objects.

All passed the stage of accreting pulsars, accelerating the rotation and decreasing the magnetic field.

Ordinary pulsars

$P=0.033 - 8 \text{ sec}$

$B= 10^{11} - 10^{13} \text{ Gauss}$

Recycled pulsars

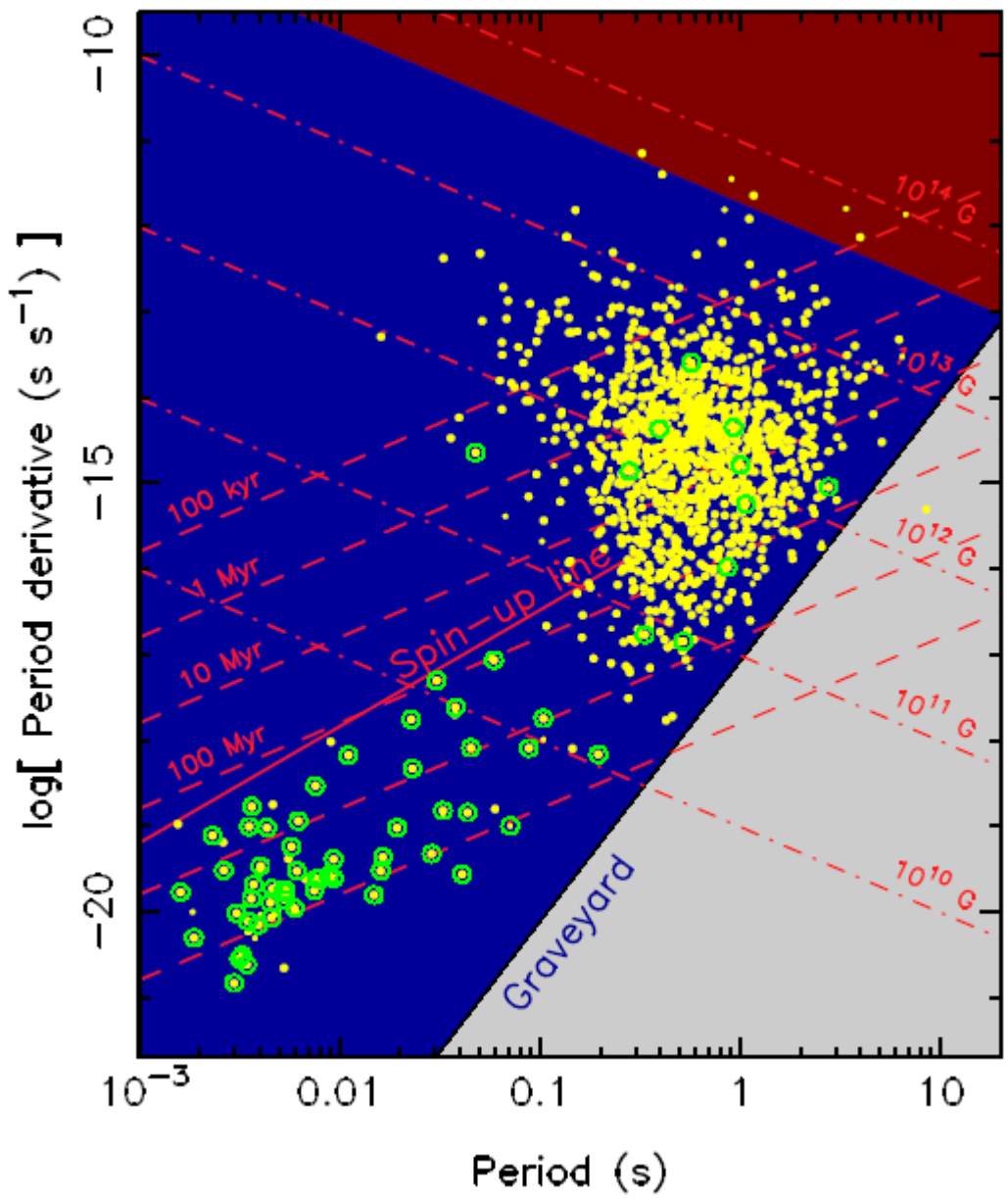
$P=1.5 - 50 \text{ msec}$

$B=10^8 - 10^{10} \text{ Gauss}$

**The P - \dot{P} diagram
shown for a sample of radio
pulsars.**

Binary pulsars are
highlighted by open circles.
Theoretical models do not
predict radio emission outside
the dark blue region.

**Lorimer (2005)
astro/ph-0511258**



Recycled pulsars: NS + WD and single - about 180 objects

NS + NS 8 objects (like Hulse- Taylor pulsar)

Single recycled pulsars (small P and B) passed the stage of X-ray pulsar in binary, and later had lost the companion WD.

NS + NS are in the Galaxy disk

NS + WD and single are in the galactic bulge, and in the globular clusters.

Globular clusters contain 0.001 of the mass of the Galaxy, and about $\frac{1}{2}$ of the recycled pulsars.

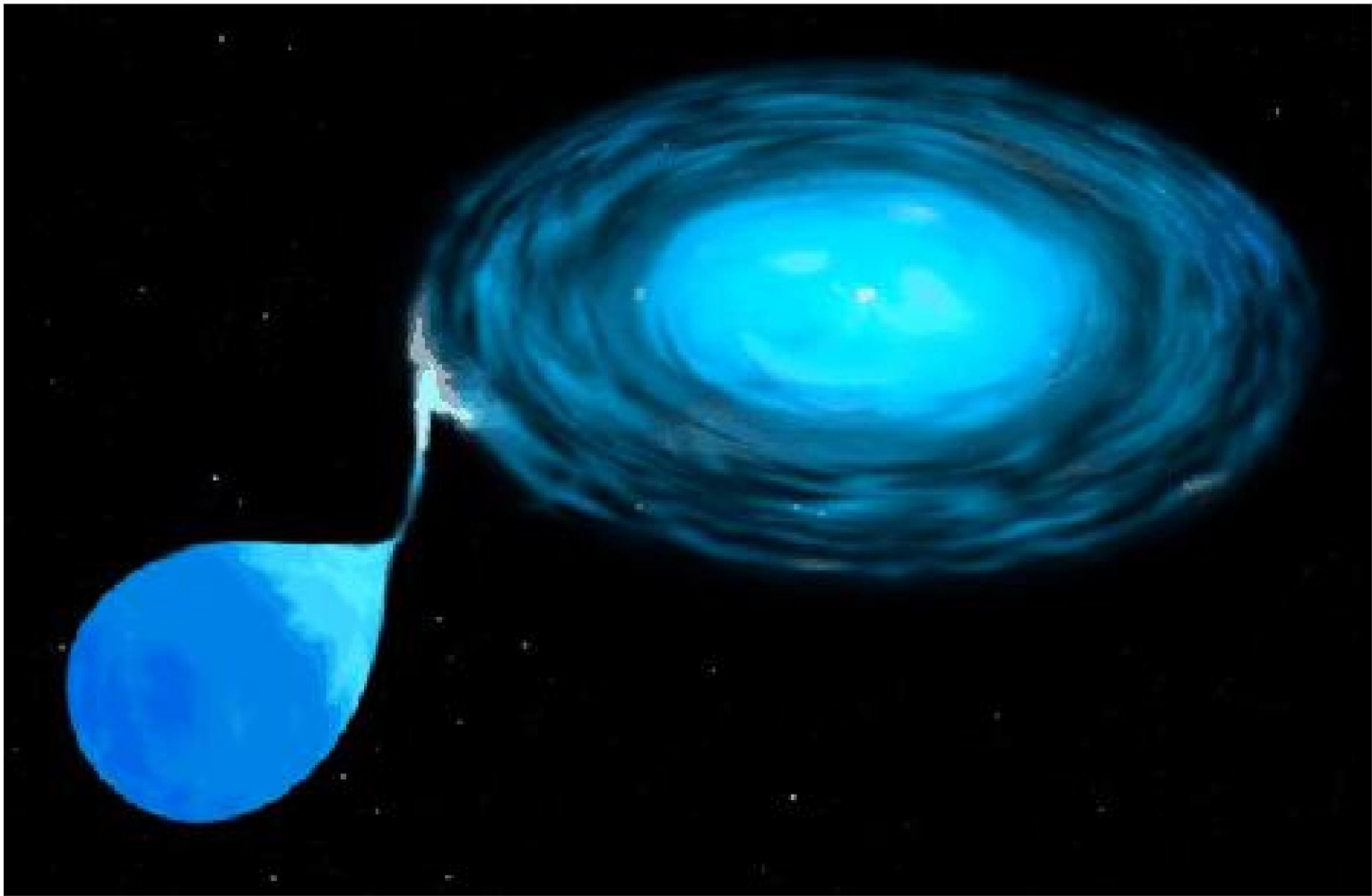
Formation of the binary in GC by tidal capture or triple collision

Disruption of the binary RP by collisions with GC stars: most single RP are situated in GC.

31 RP in Terzian 5 (11 – BP, 10 +10? – single)

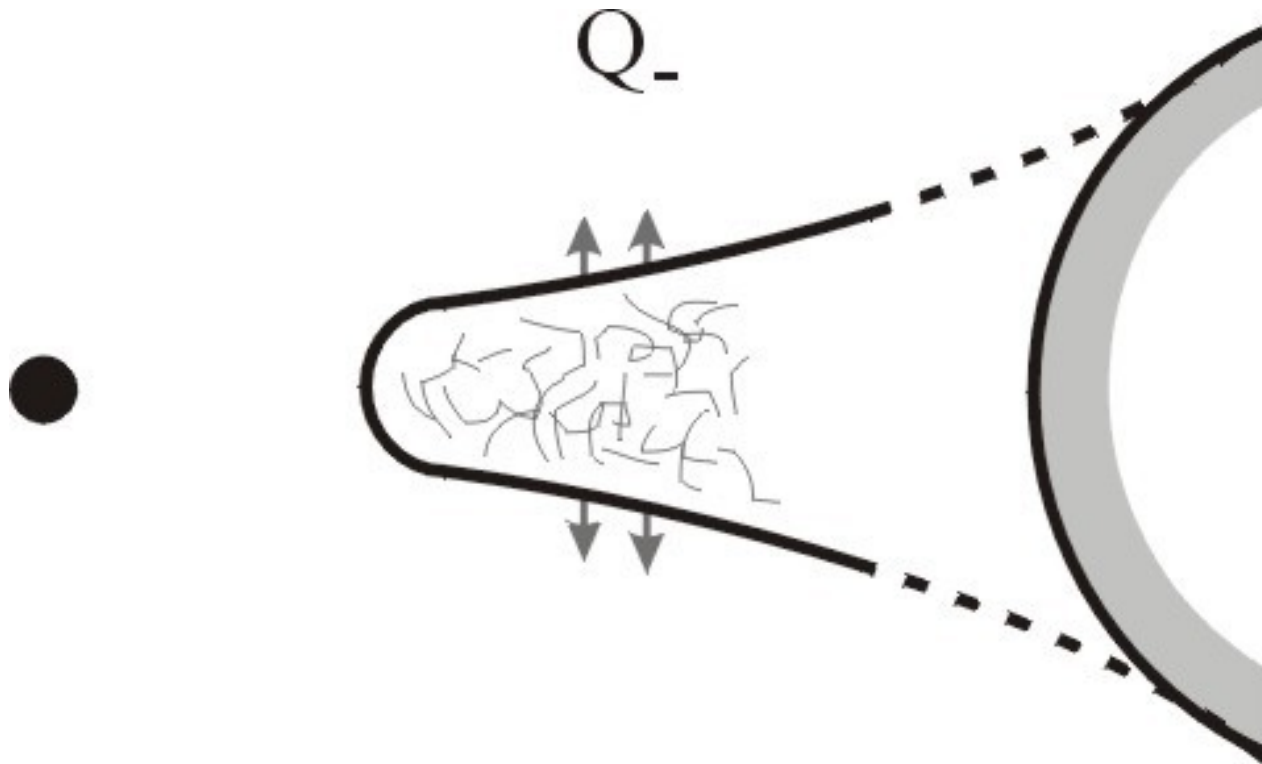
22 RP in 47 Tuc (14 – BP, 7 + 1? – single)

In total: 80 RP in Gal (15 – single), 108 RP in GC (40+15? – single)



Enhanced evaporation

Bisnovatyi-Kogan, *Astrofizika*, 32, 313 (1990)



GR Effects: NS+NS

$$\dot{\omega} = 3T_{\odot}^{2/3} \left(\frac{P_b}{2\pi} \right)^{-5/3} \frac{1}{1-e^2} (M_A + M_B)^{2/3},$$

$$\gamma = T_{\odot}^{2/3} \left(\frac{P_b}{2\pi} \right)^{1/3} e \frac{M_B(M_A + 2M_B)}{(M_A + M_B)^{4/3}},$$

$$\dot{P}_b = -\frac{192\pi}{5} T_{\odot}^{5/3} \left(\frac{P_b}{2\pi} \right)^{-5/3} \frac{\left(1 + \frac{73}{24}e^2 + \frac{37}{96}e^4 \right)}{(1-e^2)^{7/2}} \frac{M_A M_B}{(M_A + M_B)^{1/3}},$$

$$r = T_{\odot} M_B,$$

$$s = T_{\odot}^{-1/3} \left(\frac{P_b}{2\pi} \right)^{-2/3} \pi \frac{(M_A + M_B)^{2/3}}{M_B},$$

$$T_{\odot} = GM_{\odot}/c^3 = 4.925490947\mu\text{s},$$

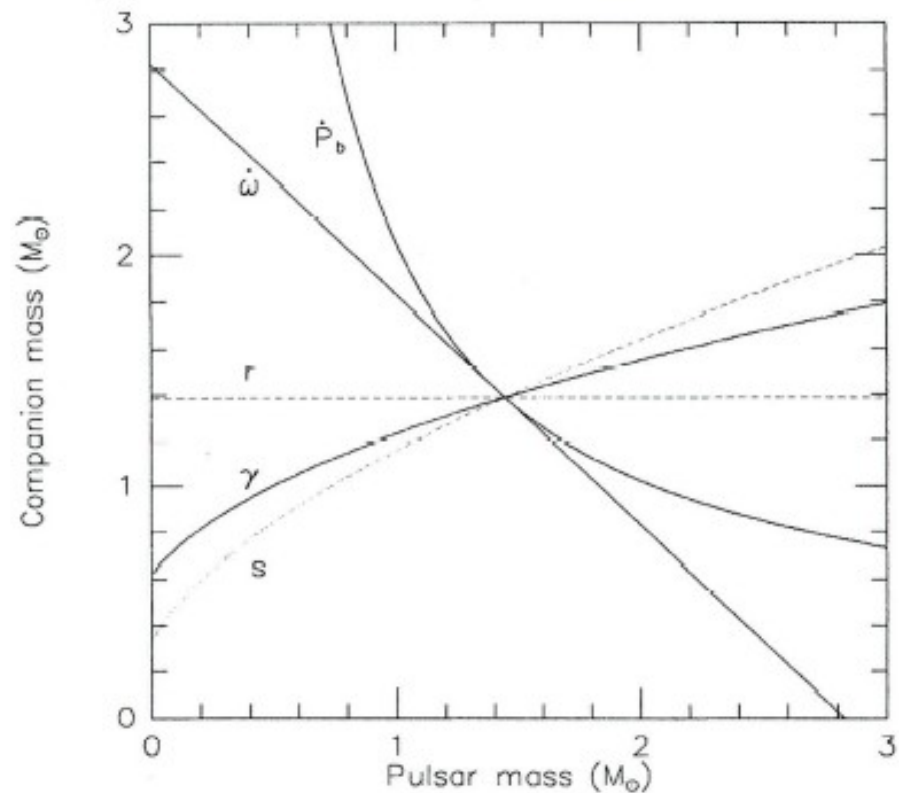


Рис. 2: Сплошные кривые соответствуют уравнениям (14-16) при учете измеренных значений $\dot{\omega}$, γ и \dot{P}_b . Пересечения этих кривых в одной точке (в пределах экспериментальной неопределенности порядка 0.35% в \dot{P}_b) устанавливает существование гравитационных волн. Штриховые линии соответствуют *предсказанным* значениям параметров r и s . Эти значения могут стать измеримыми при дальнейшем улучшении качества данных, из [96].

**PSR B1913+16 and PSR B1534+12, have provided
the best such tests so far, confirming GR at the
0.2% and 0.7% level, respectively**

NS + NS RP are the best laboratories for checking of General Relativity
1913+16 timing had shown (indirectly) the existence of gravitational waves
Nobel Prize of Hulse and Taylor (1993)

A Double-Pulsar System — A Rare Laboratory for Relativistic Gravity and Plasma Physics (Lyne et al., 2004)

The clock-like properties of pulsars moving in the gravitational fields of their unseen neutron-star companions have allowed unique tests of general relativity and provided evidence for gravitational radiation. We report here the detection of the 2.8-sec pulsar J0737-3039B as the companion to the 23ms pulsar J0737-3039A in a highly-relativistic double-neutron-star system, allowing unprecedented tests of fundamental gravitational physics. We observe a short eclipse of J0737-3039A by J0737-3039B and orbital modulation of the flux density and pulse shape of J0737-3039B, probably due to the influence of J0737-3039A's energy flux upon its magnetosphere. These effects will allow us to probe magneto-ionic properties of a pulsar magnetosphere.

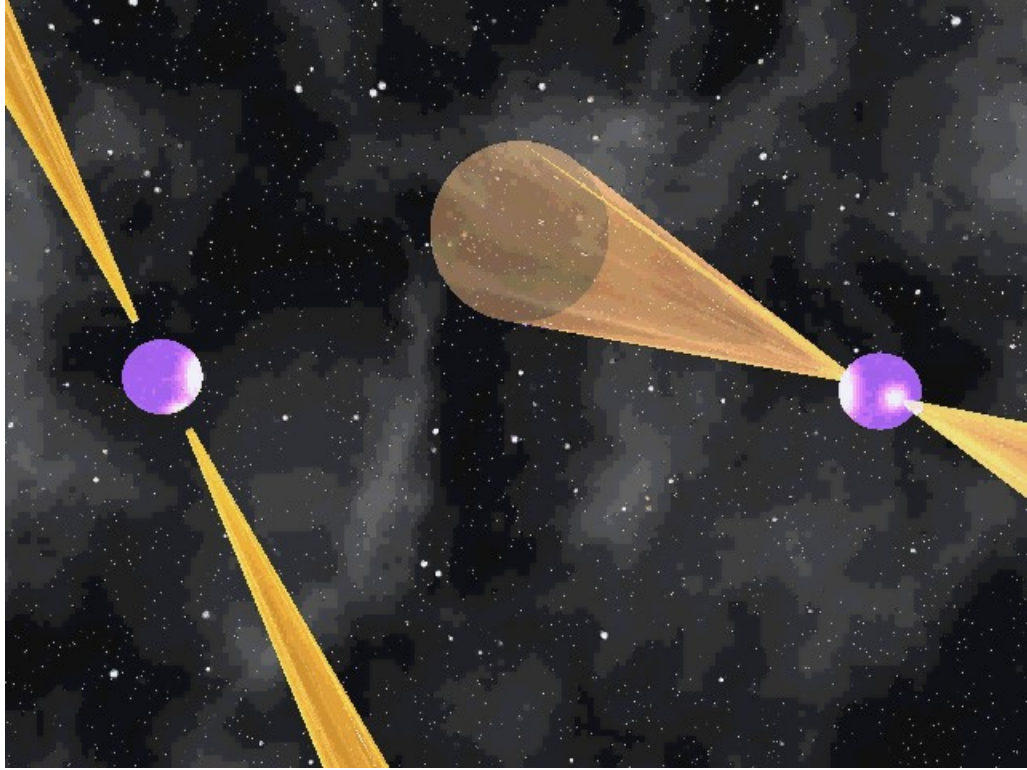


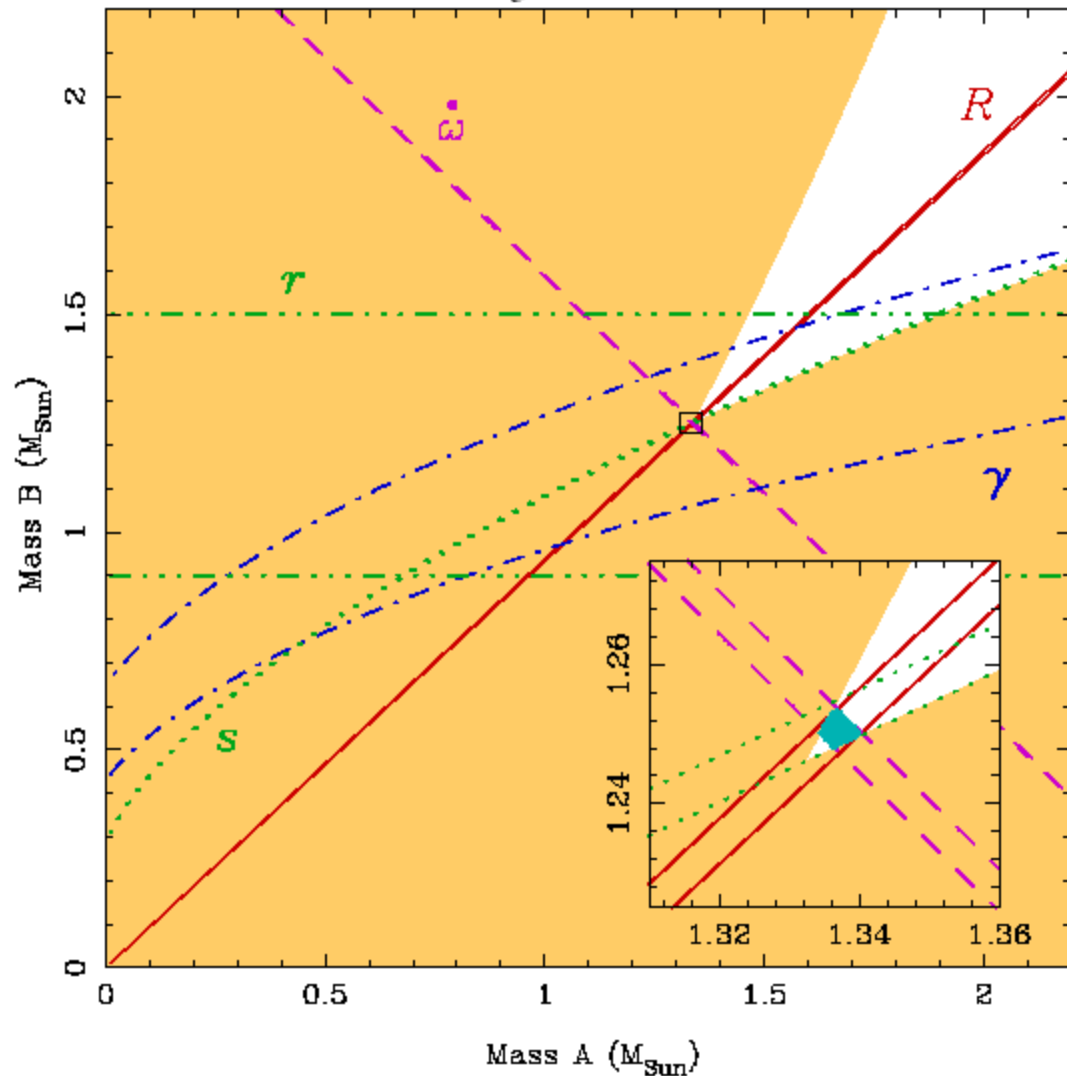
Table 1: Observed and derived parameters of PSRs J0737–3039A and B using the DD timing model (11, 13). Standard (1σ) errors are given in parentheses after the values and are in units of the least significant digit(s). The parameters A , B and δ_r in the DD model were assumed to be zero in the analysis. The distance is estimated from the dispersion measure and a model for the interstellar free electron distribution (32).

Pulsar	PSR J0737–3039A	PSR J0737–3039B
Pulse period P (ms)	22.69937855615(6)	2773.4607474(4)
Period derivative \dot{P}	$1.74(5) \times 10^{-18}$	$0.88(13) \times 10^{-15}$
Epoch of period (MJD)	52870.0	52870.0
Orbital period P_b (day)	0.102251563(1)	–
Eccentricity e	0.087779(5)	–
Epoch of periastron T_0 (MJD)	52870.0120589(6)	–
Longitude of periastron ω (deg)	73.805(3)	$73.805 + 180.0$
Projected semi-major axis $x = a \sin i/c$ (sec)	1.41504(2)	1.513(4)
Advance of periastron $\dot{\omega}$ (deg/yr)	16.90(1)	–
Gravitational redshift parameter γ (ms)	0.38(5)	–
Shapiro delay parameter s	0.9995(–32, +4)	–
Shapiro delay parameter r (μ s)	5.6(–12, +18)	–

Characteristic age τ (My)	210	50
Surface magnetic field strength B (Gauss)	6.3×10^9	1.6×10^{12}
Spin-down luminosity \dot{E} (erg/s)	5800×10^{30}	1.6×10^{30}
Mass function (M_{\odot})	0.29097(1)	0.356(3)
Distance (kpc)		~ 0.6
Total system mass $m_A + m_B$ (M_{\odot})		2.588(3)
Mass ratio $R \equiv m_A/m_B$		1.069(6)
Orbital inclination from Shapiro s (deg)		87(3)
Orbital inclination from $(R, \dot{\omega})$ (deg)		87.7(-29, +17)
Stellar mass from $(R, \dot{\omega})$ (M_{\odot})	1.337(5)	1.250(5)

Checking General Relativity

The observational constraints upon the masses m_A and m_B . The colored regions are those which are excluded by the Keplerian mass functions of the two pulsars. Further constraints are shown as pairs of lines enclosing permitted regions as ω predicted by general relativity: (a) the measurement of the advance of periastron $\dot{\omega}$, giving the total mass $m_A + m_B = 2.588 \pm 0.003 M_{\text{Sun}}$ (dashed line); (b) the measurement of $R = m_A/m_B = 1.069 \pm 0.006$ (solid line); (c) the measurement of the gravitational redshift/time dilation parameter (dot-dash line); (d) the

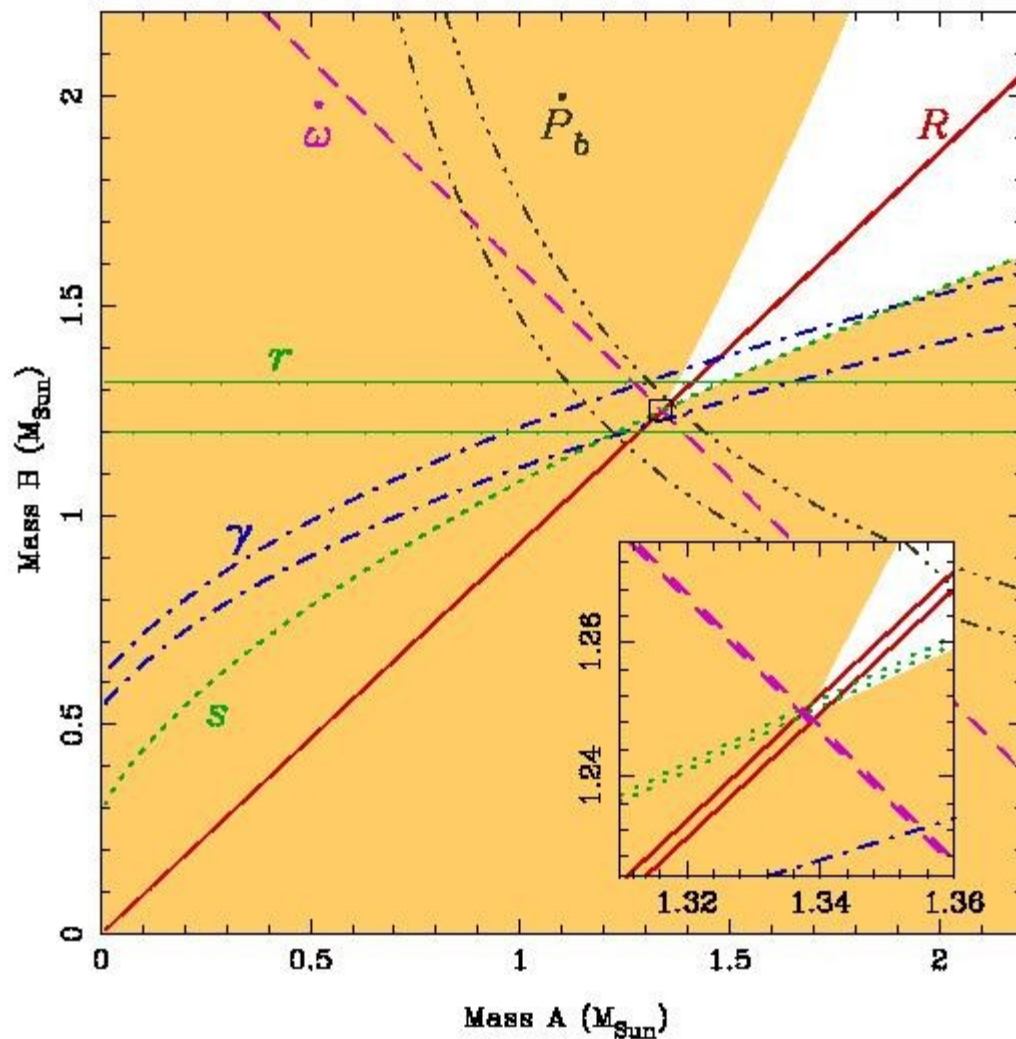


Lyne et al., 2004, Science, **303**, 1153.

TABLE I: Observed and derived parameters of PSRs J0737–3039A and B. Standard errors are given in parentheses after the values and are in units of the least significant digit(s).

Pulsar	PSR J0737–3039A	PSR J0737–3039B
Pulse period P (ms)	22.699378556138(2)	2773.4607474(4)
Period derivative \dot{P}	$1.7596(2) \times 10^{-18}$	$0.88(13) \times 10^{-15}$
Epoch of period (MJD)	52870.0	
Right ascension α (J2000)	07 ^h 37 ^m 51 ^s .24795(2)	
Declination δ (J2000)	–30° 39′ 40″.7247(6)	
Orbital period P_b (day)	0.1022515628(2)	
Eccentricity e	0.087778(2)	
Epoch of periastron T_0 (MJD)	52870.0120588(3)	
Advance of periastron $\dot{\omega}$ (deg yr ^{–1})	16.900(2)	
Longitude of periastron ω (deg)	73.805(1)	73.805 + 180.0
Projected semi-major axis $x = a \sin i / c$ (sec)	1.415032(2)	1.513(4)
Gravitational redshift parameter γ (ms)	0.39(2)	
Shapiro delay parameter $s = \sin i$	0.9995(4)	
Shapiro delay parameter r (μ s)	6.2(6)	
Orbital decay \dot{P}_b (10^{-12})	–1.20(8)	
Mass ratio $R = M_A / M_B$		1.071(1)

The observational constraints upon the masses m_A and m_B . The colored regions are those which are excluded by the Keplerian mass functions of the two pulsars. Further constraints are shown as pairs of lines enclosing permitted regions as predicted by general relativity: (a) the measurement of the advance of periastron $\dot{\omega}$, giving the total mass $m_A + m_B = 2.588 \pm 0.003 M_{\text{Sun}}$ (dashed line); (b) the measurement of $R = m_A/m_B = 1.069 \pm 0.006$ (solid line); (c) the measurement of the gravitational redshift/time dilation parameter (dot-dash line); (d) the



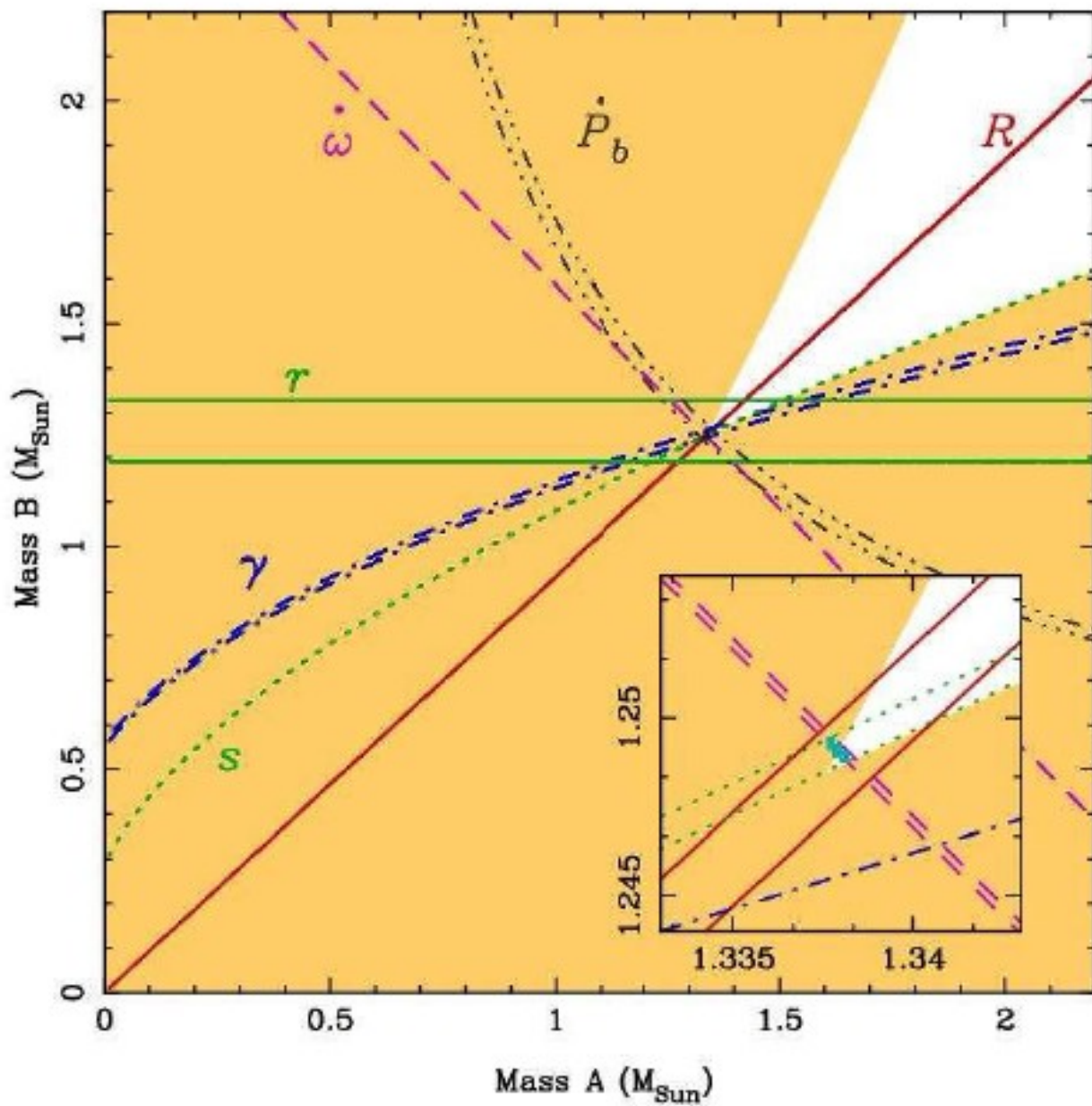
M. Kramer et al., astro-ph/0503386.

Tests of general relativity from timing the double pulsar

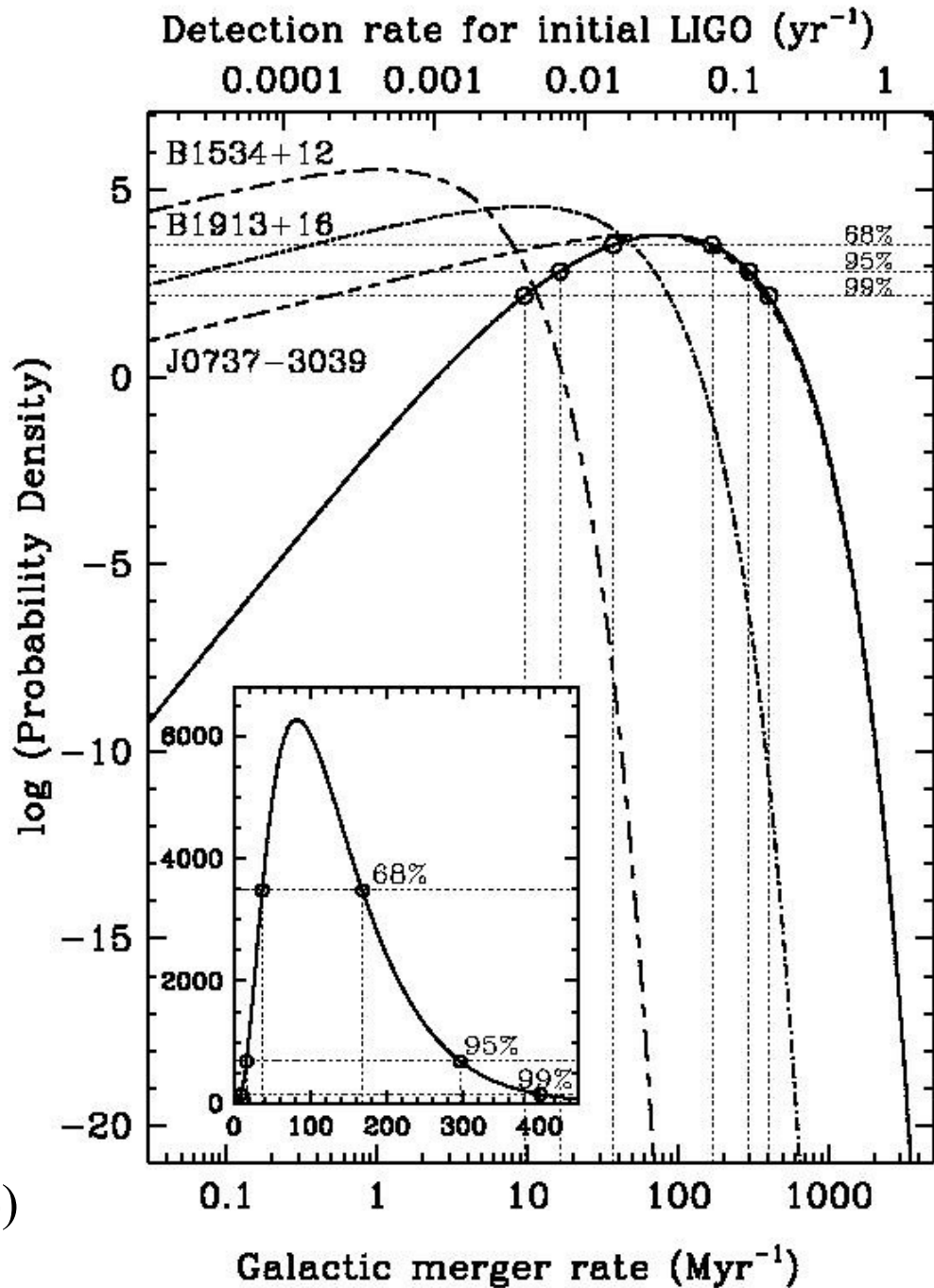
M. Kramer et al. arXiv:astro-ph/0609417, 14 Sep 2006

Here we report on precision timing observations taken over the 2.5 years since its discovery and present four independent strong-field tests of general relativity. Use of the theory-independent mass ratio of the two stars makes these tests uniquely different from earlier studies. By measuring relativistic corrections to the Keplerian description of the orbital motion, we find that the “post-Keplerian” parameter s agrees with the value predicted by Einstein’s theory of general relativity within an **uncertainty of 0.05%**, the most precise test yet obtained. We also show that the transverse velocity of the system’s center of mass is extremely small. Combined with the system’s location near the Sun, this result suggests that future tests of gravitational theories with the double pulsar will supersede the best current Solar-system tests.

Timing parameter	PSR J0737–3039A	PSR J0737–3039B
Right Ascension α	07 ^h 37 ^m 51 ^s .24927(3)	—
Declination δ	–30°39′40″.7195(5)	—
Proper motion in the RA direction (mas yr ^{–1})	–3.3(4)	—
Proper motion in Declination (mas yr ^{–1})	2.6(5)	—
Parallax, π (mas)	3(2)	—
Spin frequency ν (Hz)	44.054069392744(2)	0.36056035506(1)
Spin frequency derivative $\dot{\nu}$ (s ^{–2})	$-3.4156(1) \times 10^{-15}$	$-0.116(1) \times 10^{-15}$
Timing Epoch (MJD)	53156.0	53156.0
Dispersion measure DM (cm ^{–3} pc)	48.920(5)	—
Orbital period P_b (day)	0.10225156248(5)	—
Eccentricity e	0.0877775(9)	—
Projected semi-major axis $x = (a/c) \sin i$ (s)	1.415032(1)	1.5161(16)
Longitude of periastron ω (deg)	87.0331(8)	87.0331 + 180.0
Epoch of periastron T_0 (MJD)	53155.9074280(2)	—
Advance of periastron $\dot{\omega}$ (deg/yr)	16.89947(68)	[16.96(5)]
Gravitational redshift parameter γ (ms)	0.3856(26)	—
Shapiro delay parameter s	0.99974(–39, +16)	—
Shapiro delay parameter r (μ s)	6.21(33)	—
Orbital period derivative \dot{P}_b	$-1.252(17) \times 10^{-12}$	—
Timing data span (MJD)	52760 – 53736	52760 – 53736
Number of time offsets fitted	10	12
RMS timing residual σ (μ sec)	54	2169
Total proper motion (mas yr ^{–1})		4.2(4)
Distance $d(\text{DM})$ (pc)		~ 500
Distance $d(\pi)$ (pc)		200 – 1000
Transverse velocity ($d = 500$ pc) (km s ^{–1})		10(1)
Orbital inclination angle (deg)		88.69(–76, +50)
Mass function (M_\odot)	0.29096571(87)	0.3579(11)
Mass ratio, R		1.0714(11)
Total system mass (M_\odot)		2.58708(16)
Neutron star mass (m_\odot)	1.3381(7)	1.2489(7)



Probability density function that represents our expectation that the actual DNS binary merger rate in the Galaxy (bottom axis) and the predicted initial LIGO rate (top axis) take on particular values, given the observations. The solid line shows the total probability density along with those obtained for each of the three binary systems (dashed lines). **Inset:** Total probability density, and corresponding 68%, 95%, and 99% confidence limits, shown in a linear scale.



Kalogera V et al. *Astrophys. J. Lett.* 601 L179; 614 L137 (2004)

For the model of pulsar evolution, the mean galactic merging rate of BNS systems is $\mathbf{R} \sim 83 / \text{Myr}$. The 68%- and 95%-confidence level intervals are 40 ± 140 and $20 \pm 290 / \text{Myr}$, respectively. The expected detection rate of a gravitational-wave pulse from neighboring galaxies is 0.035 and 190 events per year for the initial (the detection limit 20 Mpc) and advanced (the detection limit 350 Mpc) LIGO interferometers, respectively. The corresponding 95%-confidence intervals are 0.007 ± 0.12 and 40 ± 660 events per year, respectively. The discovery of the double pulsar J0737-3039 increased \mathbf{R} by 6.4 times compared to earlier calculations, because it dominates in computing the total probability, as seen in Fig.

Examination of a broader class of evolutionary models of pulsars showed that in all cases, accounting for the double pulsar J0737 \pm 3039 increases the BNS merging rate by 6 - 7 times, although the rates can differ by more than 50 times in individual cases

Variability of the gravitational constant.

A. Paleontological and geophysical arguments

1. Earth surface temperature $|\dot{G}/G| < 2.0 \times 10^{-11} \text{ yr}^{-1}$

2. Expanding Earth $-\dot{G}/G \leq 8 \times 10^{-12} \text{ yr}^{-1}$.

B. Planetary and stellar orbits

$$\frac{\dot{P}}{P} = -2 \frac{\dot{G}}{G}.$$

1. Early works Moon eclipses (example)

1374 B.C. to 1715 A.D. $\dot{G}/G = (2.6 \pm 15) \times 10^{-11} \text{ yr}^{-1}$.

2. Solar system

$$\dot{G}/G = (0.0 \pm 2.0) \times 10^{-12} \text{ yr}^{-1}.$$

Variability of the gravitational constant.

The Lunar Laser Ranging (LLR) experiment has measured the position of the Moon with an accuracy of about 1 cm for 30 years.

from the first six years of LLR $|\dot{G}/G| \leq 3 \times 10^{-11} \text{ yr}^{-1}$.

20 years of data to improve this result to $|\dot{G}/G| < 1.04 \times 10^{-11} \text{ yr}^{-1}$
the main error arising from the Lunar tidal acceleration.

24 years of data concluded that $|\dot{G}/G| < 6 \times 10^{-12} \text{ yr}^{-1}$,

J. O. Dickey *et al.*, *Science* 265, 482 (1994).

Using all available astrometric data and in particular the ranging data from Viking landers on Mars,

Hellings et al., *Phys. Rev. Lett.* 51 (1983) 1609 $|\dot{G}/G| = (2 \pm 4) \times 10^{-12} \text{ yr}^{-1}$.

Variability of the gravitational constant.

Binary Recycled Pulsars

1. T.Damour, G.Gibbons, J.Taylor, PRL, 61, 1151 (1988)

Limits on the Variability of G Using Binary-Pulsar Data

One of the few experimental handles on unified theories of gravity with other interactions comes from possible time variation of coupling constants over the Hubble time: $H_0^{-1} \simeq (7.67 \times 10^{-11} \text{ yr}^{-1})^{-1}$. We present a new theory-independent estimate (consistent with zero) of the time variation of Newton's gravitational constant derived from the timing of the binary pulsar PSR 1913+16: $\dot{G}_0/G_0 = (1.0 \pm 2.3) \times 10^{-11} \text{ yr}^{-1}$. We anticipate that this estimate will become sharper as more data are acquired.

After complicated calculations: $\dot{P}_0^{\text{tot}} = \dot{P}_0^{\text{GR}} - 2P_0 \dot{G}_0/G_0$.

2. ApJ, 428, 713 (1994)

HIGH-PRECISION TIMING OF MILLISECOND PULSARS. III. LONG-TERM MONITORING OF PSRs B1885+09 AND B1937+21

V. M. KASPI,¹ J. H. TAYLOR,² AND M. F. RYBA³

$$\frac{\dot{G}}{G} = (4 \pm 5) \times 10^{-12} \text{ yr}^{-1} \quad (\text{PSR B1913} + 16)$$

$$\frac{\dot{G}}{G} = (-9 \pm 18) \times 10^{-12} \text{ yr}^{-1} \quad (\text{PSR B1855} + 09).$$

Checking the variability of the gravitational constant with binary pulsars

PSR B1913+16

Table 1: Error budget for the orbital period derivative, in comparison with the general relativistic prediction, from [10].

	Parameter	(10^{-12})
Observed value	\dot{P}_b^{obs}	-2.4225 ± 0.0056
Galactic contribution	\dot{P}_b^{gal}	-0.0124 ± 0.0064
Intrinsic orbital period decay	$\dot{P}_b^{obs} - \dot{P}_b^{gal}$	-2.4101 ± 0.0085
General relativistic prediction	\dot{P}_b^{GR}	-2.4025 ± 0.0001

J.H. Taylor,
Classical and
Quantum
Gravity 10
(1993) 167.

$$\frac{\dot{G}}{G} = -\frac{1}{2} \frac{\dot{P}_b}{P_b}, \quad \frac{\delta e}{e} = 0, \quad e = \text{const.}$$

Bisnovatyi-Kogan, gr-qc/0511072

RP PSR B1913+16 (1992)

$$\frac{\dot{G}}{G} = (4.3 \pm 4.9) \cdot 10^{-12} \text{ yr}^{-1}.$$

better precision is expected from timing of **RP J0737-3039A**

The orbital decay, \dot{P}_b is measured at the 1.4% level after only 2.5 years of timing, corresponds to a shrinkage of the pulsars' separation at a rate of 7mm per day.

The combination of Mariner 10 and Mercury and Venus ranging data gave (1992)

$$\dot{G}/G = (0 \pm 2) \cdot 10^{-12} \text{yr}^{-1}$$

Combining with binary pulsar data we obtain

Bisnovatyi-Kogan, gr-qc/0511072

\dot{G}/G inside the limits $(-0.6 \div +2) \cdot 10^{-12} \text{ year}^{-1}$

Recent results

Lunar Laser Ranging Tests of Relativistic Gravity

Williams et al. gr-qc/0411113

$$\dot{G}/G = (4 \pm 9) \times 10^{-13} \text{ yr}^{-1}$$

Lunar Laser Ranging Contributions to Relativity and Geodesy

J. Mueller, J. G. Williams, S. G. Turyshev **gr-qc/0509114**

Time varying gravitational constant \dot{G}/G [yr ⁻¹]		$(6 \pm 8) \cdot 10^{-13}$	
---	--	----------------------------	--

GR improving the accuracy to $\sim 0.05\%$

Incompletely modeled solid Earth tides, ocean loading or geocenter motion, and uncertainties in values of fixed model parameters have to be considered in those estimations.

CONCLUSIONS

1. Timing of the pulsars **J0737-3039A /B** is the most powerful instrument for the verification of General Relativity due to unprecedented precision of the observation
2. Recycled pulsars are the most precise available time standards
3. GW radiated during merging of NS have a chance to be registered by LIGO
4. Future tests of gravitational theories with the double pulsar will supersede the best current Solar-system tests.
5. Checking the physics beyond the standard: G-variability

**Most Accurate Time
measurements by REcycled
pulsars
(MATRE- Space Watch)**

**Самые точные
измерения времени с
помощью подкрученных
пульсаров
(МЭТР – Космические
часы)**

